



6th Intercontinental Geoinformation Days

igd.mersin.edu.tr



Comparison of different land surface temperature (LST) estimation algorithms using remotely sensed images

Ali Hosingholizade ¹, Parviz Zeaiean Firouzabadi ² Foroogh Khazaei Nezhad ³ Mozhban Dehghani Aghchekohal ²

¹University of Tehran, Geography, Remote sensing and GIS, Tehran, Iran

²Kharazmi University, Geography, Remote sensing and GIS, Tehran, Iran

³Kosar University of Bojnord, Humanities, Geography, Bojnord, Iran

Keywords

Remote sensing
LST
Emissivity
Stefan_Boltzman
Tehran

Abstract

Earth Surface Temperature is a key indicator of energy balance on Earth. In recent years, several methods for obtaining temperature using satellite images have been provided. This study aimed to compare the performance of different methods to estimate Land Surface Temperature (LST). Here, LST over Tehran metropolitan city has been estimated through three methods including Artis, Mono_window and Stefan_Boltzman algorithms applied to Landsat (TM, ETM+, OLI) and MODIS image, Emissivity obtained through image classification, the vegetation index (NDVI) and MODIS emissivity product. Then, using an accurate thermometer, surface and air temperature at a height of one and a half meters were taken. The linear relationship between surface temperature and corresponding air temperature has been established. A statistical measure namely mean absolute error and T test for selection of best method were used. The results show that Stefan_Boltzman method with mean absolute error of 1.540 °C was the best one. Therefore, it is suggested that the Stefan_Boltzman method be used for other areas with the same weather conditions and geographical parameters.

1. Introduction

Today, with the expansion of urban areas, accurate thermal data are essential for managing, designing and planning cities (Deng et al. 2023; Sidiqi et al. 2016). Analysing the trend of existing hot spots can have a direct impact on the design of new urban fabric and the process of renovation of old fabrics, especially in developed countries (Mullerova and Williams, 2019). Progress and development in remote sensing technology has made it possible to extract accurate thermal data from urban environments, which has drawn many researchers' attention to this issue and its different methods in cities (Orusa and Mondino, 2019).

Selection of accurate method to obtain temperature, even in a wider dimension, is an important factor in the study of global changes as a heat balancer and controller of climate models (Halder et al. 2021; Sidiqi et al. 2016). The knowledge of the surface temperature is very important for a wide range of issues in earth sciences, including the temperature of different regions, wide changes and interactions between human activities and

the surrounding environment (Perera et al. 2022). Although the temperature difference in different regions may not be very large, this small amount can cause many disorders (Shang and Dick. 2006).

To date, various algorithms have been provided to obtain the temperature of the earth's surface. From methods that are based on classifying NDVI through thresholding (Guha et al. 2018; Hosingholizade et al. 2021) to the use of MODIS ready products (Yu et al. 2022) and other relatively older methods such as station-based observations interpolation and the use of mobile stations that do not consider the emission and instead use special thermometers to calculate the air temperature (Ozelkan et al. 2015). Since last years, various formulas have been presented to calculate the temperature. Each formula is used separately. (Mia et al. 2014).

The aim of this study is to find the best method in estimating surface temperature via comparison different methods.

The results of this research can significantly enhance the knowledge of scientists in estimation of earth surface temperature with different algorithms.

* Corresponding Author

(a.hosingholizade@ut.ac.ir) ORCID ID 0000-0001-5286-1361
(zeaeian@khu.ac.ir) ORCID ID 0000-0001-8407-5605
(f.khazaei@kub.ac.ir) ORCID ID 0000-0000-0000-0000
(Dehghanim848@gmail.com) ORCID ID 0000-0000-0000-0000

Cite this study

Hosingholizade A, Zeaiean Firouzabadi P, Khazaei Nezhad F & Dehghani aghchekohal M (2023). Comparison of different land surface temperature (LST) estimation algorithms using remotely sensed images. Intercontinental Geoinformation Days (IGD), 6, 305-308, Baku, Azerbaijan

2. Method

2.1. Study area

The studied area is a part of Tehran province in latitude°35°20 to°36°00'N and longitude°50°48 to°52°E. This region has a lot of diversity in terms of climate. It starts from the desert climate in the southern parts and continues to the humid climate in the north and mountainous in the eastern parts. In terms of the UTM classification system, it is also in the 39th North zone, and its height ranges from 1050 in the South to 1800 meters in the North.

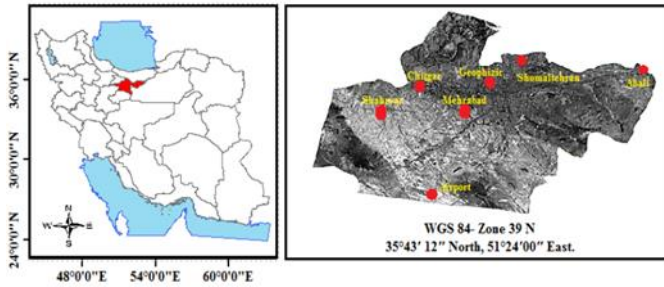


Figure 1. Iran (left)and Theran seven synoptic stations(right)

Table 1. Geographical coordinates of stations

NO	Station	Latitude	Longitude
1	Chitgar	35 44	51 10
2	Mehrabad	35 41	51 19
3	Airport	35 25	51 10
4	Abali	35 44	51 53
5	Geophizic	35 45	51 23
6	Shahryar	35 40	51 02
7	Shomal Tehran	35 48	51 29

2.2. Data

In this research, images of TM, ETM+ and TIRS sensors and the ready product of MODIS satellite, meteorological data including air temperature (Ta) and relative humidity (RH) data as well as surface and air temperature of some sample points were used. The number of rows and paths used for all images are 35 and 164, respectively. It was also tried to select images with the least amount of cloud to avoid malfunction of different algorithms.

2.2.1. Estimation of temperature from emissivity based on classification

Here, using the SVM method, the image was divided into 6 separate classes and each class was assigned an emissivity based on available scientific sources. Finally, the emissivity map entered to the surface temperature estimation algorithms. (Chen, 2015).

Table 2. Emissivity of different classes

NO	Class	Emissivity
1	Water	0.992
2	Soil	0.962
3	Aqriculture	0.942
4	Dence Cover	0.975
5	Cover non-Cindensing	0.924
6	Urban	0.918

2.2.2. Estimating temperature from emissivity based on NDVI

After calculating NDVI, a specific emissivity value was given to each NDVI interval based on different formulas presented in Table 3 (Zhang et al. 2006).

Table 3. Division of NDVI ranges

NO	NDVI	Emissivity
1	-1<NDVI<-0.185	0.985
2	-0.185<NDVI<+0.157	0.955
3	+0.157<NDVI<0.727	1.0094 + 0.047ln (NDVI)
4	+0.727<NDVI<+0.8	0.99
5	+0.8<NDVI<1	0.99

2.2.3. Estimation of temperature with emissivity obtained from MODIS ready product

In this method, using bands 31 and 32 MODIS satellite, which is special for emission and has a pixel size of one kilometer, and resampling this product to reach a pixel size of 30 meters and enter it into the temperature estimation equations, the land surface temperature of the earth is calculated.

2.3. Mono-window

In Mono-Window algorithm, spectral radiance for each band is obtained with the following relationship (Eq. 1-7), gain and offset can be extracted from the attached Header File and follow the rest of the steps with the following relationships.

$$L_{\lambda} = \text{gain} \times \text{DN} \times \text{offset} \tag{1}$$

$$L_{\lambda} = \frac{L_{\max} - L_{\min}}{Qcal_{\max} - Qcal_{\min}} \times (DN - Qcal_{\min}) + L_{\min} \tag{2}$$

$$T_{\text{sensor}} = \frac{K_2}{\ln\left(\frac{K_1}{L_{\lambda}} + 1\right)} \tag{3}$$

$$W_i = 0.0981 \times \left\{ 10 \times 0.6108 \times \exp\left[\frac{17.27 \times (T_0 - 273.15)}{237.3 + (T_0 - 273.15)}\right] \times (RH/100) \right\} + 0.1697 \tag{4}$$

$$D = (1 - \tau_i) \times [1 + (\epsilon_i \times \tau_i)] \tag{5}$$

$$C = \epsilon_i \times \tau_i \tag{6}$$

$$T_s = \frac{\{a(1 - C - D) + [b(1 - C - D) + C + D] \times T_{\text{sensor}} - (D \times T_a)\}}{C} \tag{7}$$

Table 4. Estimating τ_i based on W_i

Temperature	W_i	τ_i equation
High	0.4 - 1.6	0.97429 - 0.08007 W_i
High	1.6 - 3	1.031412 - 0.11536 W_i
Low	0.4 - 1.6	0.982007 - 0.09611 W_i
Low	1.6 - 3	1.05371 - 0.14142 W_i

Where, K1 and K2 First and second calibration constant. L_λ Spectral radiance. BT Effective temperature (Kelvin). W_i water vapor. T_0 Air temperature. RH relative humidity. $a=-67.355351$, $b=0.458606$. T_s Earth surface temperature. ε_i Emissivity. τ_i Air permeability.

2.4. Artis method

After calculating the spectral radiance, the brightness temperature at the measuring surface and the emissivity with the Normalized Differential Vegetation Index (NDVI), the MODIS classification or ready product, surface temperature is obtained by this method, is calculated using the following formula (Eq. 8) (Tan et al., 2010).

$$S_t = \frac{T_{\text{sensor}}}{1 + (\lambda \times (T_{\text{sensor}} / \rho)) \text{Ln} \varepsilon} \quad (8)$$

2.5. Stefan-Boltzmann method

Thermal infrared sensors measure the radiation in the upper part of the atmosphere (Top Of Atmosphere), which is called the brightness temperature (as well as the black body temperature), which is obtained using the Equation 9-11.

$$B_\lambda = \frac{C_1}{\lambda^5 \exp\left(\frac{C_2}{\lambda \times T}\right) - 1} \quad (9)$$

$$TB = \left(\frac{1}{\text{Ln}\left(\frac{2hc^2\lambda^{-5}}{B_\lambda} + 1\right)} \right) \left(\frac{hc}{kh} \right) \quad (10)$$

$$T_s = \frac{T_B}{\sqrt[4]{\varepsilon}} \quad (11)$$

Where, $C_1 = 1.19104 \times 10^8$, $C_2 = 14387.7$, $h = 6.62 \times 10^{-34}$, $C = 2.998 \times 10^8$, $K = 1.38066 \times 10^{-23}$, $B_\lambda =$ Blackbody radiation

3. Results

Hourly meteorological data of synoptic stations in Tehran city were used to calculate the parameters related to temperature extraction. Considering that the time of taking the images is approximately 6:00 a.m. Greenwich time and the time difference between Greenwich and Tehran time is three and a half hours, the data related to 6:00 a.m. (GMT) of Tehran synoptic stations were used. These data include temperature and relative humidity data that were prepared from the Iranian Meteorological Organization. After calculating the temperature by the mentioned methods, their RMS error values were presented as described in the following table (Table 5).

Table 5. Error rate (Celsius) of temperature calculation after conversion to air temperature

	Mono Window	Artis	Stefan Boltz
TM 2010/6/4	1.56	1.70	1.42
ETM 2002/8/9	2.17	1.81	1.52
TIRS 2015/9/6	2.19	2.16	1.74
TM 2008/6/30	1.43	1.35	1.28
TM 2009/7/19	2.30	2.12	1.98
ETM 2002/10/12	1.50	1.14	1.09
ETM 2001/6/30	1.98	1.93	1.75
ETM 2002/10/12	1.58	1.39	1.26
TM 2010/6/4	1.99	1.72	1.5
TIRS 2015/9/6	1.62	1.39	1.14
ETM 2001/6/03	2.05	1.66	1.59
ETM 2002/8/9	1.52	1.44	1.34
TM 2008/6/30	1.64	1.4	1.35
TM 2009/7/19	2.16	2.09	1.82
MODIS 2009/6/30	1.95	1.65	1.48
MODIS 2009/7/19	2.37	2.25	2.22
MODIS 2015/9/6	2.64	2.49	2.38

4. Discussion

In this research, the methods of single window, Stefan-Boltzman and Landsat Science Office were used in TM, TIRS(OLI), ETM+ images. Then the results were analyzed using statistical methods. The influential parameter in estimating the best value of the earth's surface temperature is the radiation power, which is calculated in the first method through NDVI for each separate image, which is separate and constant in all stages of using the three methods mentioned for each image, and in the second method, the emissivity from the obtained classification method is calculated for each image separately, and for this method, it is separate and fixed in all stages of using the three methods mentioned for each image. Eventually in the third method "MODIS ready products" were used.

The results of all the methods were compared on different dates using the widely used statistical measure of mean absolute error. The results showed that among the methods used, the best method in estimating the temperature of the earth's surface closer to the ground data of air temperature in all three gauges and in three modes of obtaining the amount of emissivity (NDVI method, classification and MODIS ready product) The Stefan-Boltzman method had the best results, so that among the methods used, the values of the average absolute error index for the three single-window methods, Artis and Stefan-Boltzman were 1.877, 1.744 and 1.540 degrees Celsius, respectively. Therefore, it is suggested that for other areas that Use this method if it is close to the study area in terms of weather conditions and other geographical parameters.

5. Conclusion

Considering that temperature is a fleeting and highly variable quantity, the algorithm used to estimate it should be chosen correctly. Also, in addition to the type of algorithm, the emissivity estimation method directly affects the output result. On the other hand, by calculating Sig (significance level) which is considered 0.05 in the t-test, it is more than 5 percent in all methods,

which indicates that the results obtained from our samples is suitable for larger values. In other words, the results can be generalized to other samples. Therefore, it is suggested to use the appropriate method in the areas that have the same conditions as our study area, according to the purpose of the research and the existing conditions.

Acknowledgement

The authors would like to thank the Department of RS and GIS, Kharazmi University, Tehran.

References

- Chen, C. (2015). Determining the Leaf Emissivity of Three Crops by Infrared Thermometry. *Sensors*, 15(5), 11387-1140. <https://doi.org/10.3390/s150511387>
- Deng, X., Gao, F., Liao, S., Liu, Y., & Chen, W. (2023). Spatiotemporal evolution patterns of urban heat island and its relationship with urbanization in Guangdong-Hong Kong-Macao greater bay area of China from 2000 to 2020. *Ecological Indicators*, 146, 109817. <https://doi.org/10.1016/j.ecolind.2022.109817>
- Guha, S., Govil, H., Dey, A., & Gill, N. (2018). Analytical study of land surface temperature with NDVI and NDBI using Landsat 8 OLI and TIRS data in Florence and Naples city, Italy. *European Journal of Remote Sensing*, 51(1), 667-678. <https://doi.org/10.1080/22797254.2018.1474494>
- Halder, B., Bandyopadhyay, J., & Banik, P. (2021). Evaluation of the climate change impact on urban heat island based on land surface temperature and geospatial indicators. *International Journal of Environmental Research*, 15(5), 819-835. <https://doi.org/10.1007/s41742-021-00356-8>
- Hossingholizade, A., Zeaiean, P., & Beyranvand, P. (2021). Comparison of Different Retrieval Temperature algorithms With different Emissivity by Using remote sensing images. *Geographic Space*, 20(72), 39-56.
- Mia, M. B., Nishijima, J., & Fujimitsu, Y. (2014). Exploration and monitoring geothermal activity using Landsat ETM+ images: A case study at Aso volcanic area in Japan. *Journal of Volcanology and Geothermal Research*, 275, 14-21. <https://doi.org/10.1016/j.jvolgeores.2014.02.008>
- Mullerova, D., & Williams, M. (2019). Satellite monitoring of thermal performance in smart urban designs. *Remote Sensing*, 11(19), 2244. <https://doi.org/10.3390/rs11192244>
- Orusa, T., & Mondino, E. B. (2019, October). Landsat 8 thermal data to support urban management and planning in the climate change era: A case study in Torino area, NW Italy. In *Remote Sensing Technologies and Applications in Urban Environments IV* (Vol. 11157, pp. 133-149). SPIE. <https://doi.org/10.1117/12.2533110>
- Ozelkan, E., Bagis, S., Ozelkan, E. C., Ustundag, B. B., Yucel, M., & Ormeci, C. (2015). Spatial interpolation of climatic variables using land surface temperature and modified inverse distance weighting. *International Journal of Remote Sensing*, 36(4), 1000-1025. <https://doi.org/10.1080/01431161.2015.1007248>
- Perera, T. A. N. T., Nayanajith, T. M. D., Jayasinghe, G. Y., & Premasiri, H. D. S. (2022). Identification of thermal hotspots through heat index determination and urban heat island mitigation using ENVImet numerical micro climate model. *Modeling Earth Systems and Environment*, 8(1), 209-226. <https://doi.org/10.1007/s40808-021-01091-x>
- Shang, L., & Dick, R. P. (2006). Thermal crisis: challenges and potential solutions. *IEEE Potentials*, 25(5), 31-35. <https://doi.org/10.1109/MP.2006.1692283>
- Sidiqui, P., Huete, A., & Devadas, R. (2016, July). Spatio-temporal mapping and monitoring of Urban Heat Island patterns over Sydney, Australia using MODIS and Landsat-8. In *2016 4th International Workshop on Earth Observation and Remote Sensing Applications (EORSA)* (pp. 217-221). IEEE. <https://doi.org/10.1109/EORSA.2016.7552800>
- Tan, K., Lim, H., Matjafri, M., & Abdullah, K. (2010). Land surface temperature retrieval by using ATCOR3_T and normalized difference vegetation index methods in Penang Island. *American Journal of Applied Sciences*, 7(5), 717.
- Yu, P., Zhao, T., Shi, J., Ran, Y., Jia, L., Ji, D., & Xue, H. (2022). Global spatiotemporally continuous MODIS land surface temperature dataset. *Scientific Data*, 9(1), 1-15. <https://doi.org/10.1038/s41597-022-01214-8>
- Zhang, J., Wang, Y., & Li, Y. (2006). A C++ program for retrieving land surface temperature from the data of Landsat TM/ETM+ band6. *Computers & Geosciences*, 32(10), 1796-1805. <https://doi.org/10.1016/j.cageo.2006.05.001>